JTTEE5 20:48–58
DOI: 10.1007/s11666-010-9537-5
1059-9630/$19.00 © ASM International

Peer Reviewed

Effect of Substrate Temperature and Ambient Pressure on Heat Transfer at Interface Between Molten Droplet and Substrate Surface

M. Fukumoto, K. Yang, K. Tanaka, T. Usami, T. Yasui, and M. Yamada

(Submitted April 30, 2010; in revised form June 22, 2010)

Millimeter-sized molten Cu droplets were deposited on AISI304 substrate surface by free falling experiment. The roles of substrate temperature and ambient pressure on heat transfer at interface between molten droplet and substrate surface were systematically investigated. The splat characteristics were evaluated in detail. Temperature history of molten droplet was measured at splat-substrate interface. Cooling rate of the flattening droplet was calculated as well. Furthermore, the spreading behavior of molten droplet on substrate surface was captured by high speed camera. The heat transfer from splat to substrate was enhanced both by substrate heating and by ambient pressure reduction, which can be attributed to the good contact at splat bottom surface. The splats in free falling experiment showed similar changing tendency as thermal-sprayed particles. Consequently, substrate temperature and ambient pressure have an equivalent effect to contact condition at interface between droplet and substrate surface. Substrate heating and pressure reduction may enhance the wetting during splat flattening, and then affect the flattening and solidification behavior of the molten droplet.

Keywords ambient pressure, contact, free falling, heat transfer, substrate temperature, wetting

1. Introduction

Coating is a covering that is applied to the surface of an object, usually referred to as the substrate. In many cases, coatings are applied to improve surface properties of the substrate, such as appearance, adhesion, wettability, corrosion resistance, wear resistance, and scratch resistance. In other cases, in particular in printing processes and semiconductor device fabrication, the coating forms an essential part of the finished product. Thermal spraying is a process that can provide thick coatings over a large area at high deposition rate as compared to other coating processes. Up to now, this technique is widely used in many industrial applications: mechanics, aeronautics, aerospace, chemistry and oil, electronic, military, automotive, medical, marine, and mining, and their development has continuously increased over the last decade (Ref 1-3). It is, however, pointed out that the controllability or reliability of the process has not been established yet until today. As the flattening of an individual thermal-sprayed particle on the substrate is a fundamental process for the coating formation, coating microstructure, and corresponding properties, such as porosity and adhesion strength, depend strongly on the flattening nature of each splat (Ref 4). In order to establish the process controllability, it is necessary to study in detail the basic process of flattening behavior of the sprayed particles, not only for scientific interest, but also as technical consequences.

A transition phenomenon in the flattening behavior of the thermal-sprayed particles on the flat substrate surface was introduced by the authors (Ref 5, 6), which reported that when the substrate temperature is increased, the splat shapes of most materials sprayed onto flat substrates undergoes a transition from a distorted shape with splash to a disk one. It is quite interesting and practically meaningful, because the adhesion strength of the coating changed transitionally with the substrate temperature increasing, and its dependence on the substrate temperature corresponded well to that of the splat pattern (Ref 4, 7). Moreover, existence of a similar transition phenomenon in the flattening behavior of the thermal-sprayed particles on the flat substrate surface was introduced recently (Ref 8-11), i.e., the transition occurs by reducing the ambient pressure in deposition chamber.

This article is an invited paper selected from presentations at the 2010 International Thermal Spray Conference and has been expanded from the original presentation. It is simultaneously published in *Thermal Spray*: *Global Solutions for Future Applications, Proceedings of the 2010 International Thermal Spray Conference*, Singapore, May 3-5, 2010, Basil R. Marple, Arvind Agarwal, Margaret M. Hyland, Yuk-Chiu Lau, Chang-Jiu Li, Rogerio S. Lima, and Ghislain Montavon, Ed., ASM International, Materials Park, OH, 2011.

M. Fukumoto, K. Yang, K. Tanaka, T. Usami, T. Yasui, and **M. Yamada**, Department of Mechanical Engineering, Toyohashi University of Technology, Toyohashi, Aichi 441-8580, Japan. Contact e-mail: fukumoto@tut.jp.

In general, there are so many relating factors in the splat formation process which has been extensively investigated by theoretical (Ref 12, 13), numerical simulation (Ref 14-16), and experimental methods (Ref 17-20) in the last few decades. Moreover, the Sommerfeld number K based on the study of water and ethanol droplet, has been often mentioned recently (Ref 21, 22), which is described in Eq 1

$$K = We^{1/2}Re^{1/4} \quad \text{(Eq 1)}$$

where We and Re are Weber number and Reynolds number, respectively. If $K < 3$, splat rebounds; while $3 < K < 57.7$, it results in deposition; and, if $K > 57.7$, it induces splashing. However, for thermal spraying conditions involved in particle solidification, these critical values seem not applicable. Significant splashing occurred even the K is smaller than the critical value of 57.7 when alumina particles were thermally sprayed onto the stainless steel substrate (Ref 23). While in Li's study, nearly all the plasma-sprayed particles yield a K from several hundreds to thousands, which is quite higher than the critical value, but the splats deposited by those particles on preheated substrate always displayed a disk-shape without any splashing (Ref 24). These results indicated that the model is not enough to clarify the splat formation process of the thermal-sprayed particles.

Shortly speaking, the splat formation process of the thermal-sprayed particles is not fully understood yet, we still cannot answer why or how does disk-shaped splat appear, and what is the essential of the flattening problem? Therefore, there is a need for a detail study of this aspect. However, thermal spraying is a complex and short-period process, it is difficult to clarify the flattening behavior of the thermal-sprayed particles directly with current technology. Therefore, a free falling experiment was carried out as a model of the thermal spray process, using both experiments and numerical simulation (Ref 25-31). The relating factors, such as, thermal contact resistance and the droplet velocity at impact were investigated carefully. According to their study, the thermal contact resistance is determined by the area of contact between the molten droplet and the rough solid substrate (Ref 28). Furthermore, the number of fingers formed around the droplet increased with impact velocity (Ref 28, 31). However, low melting point droplet materials were used in their study (Ref 28-31), these materials may not applicable for the practical usage of the thermal spraying process.

In this study, the flattening and solidification behavior of the free falling Cu droplet onto AISI304 substrate were systematically investigated by controlling substrate temperature and ambient pressure in deposition chamber, respectively. This article focuses, in particular, on the heat transfer at interface between molten droplet and substrate surface. In addition, the characteristics of the individual splat were evaluated precisely.

2. Experimental Procedures

2.1 Raw Materials and Free Falling Apparatus

Millimeter-sized molten Cu droplets were deposited on AISI304 substrate surface by free falling experiment. Commercially available Cu wire with a diameter of 2 mm (99.9% pure) was used as droplet material; the physical properties of Cu droplet are summarized in Table 1. All the values were measured at the melting temperature of Cu droplet, except the thermal conductivity (Ref 32). AISI304 plate with dimensions of 30 × 30 × 5 mm was used as substrate, the chemical compositions of AISI304 substrate are presented in Table 2. Substrate surface was finally polished with No. 2000 sandpaper prior to the experiment. A part of the substrates were heated in air by the experiment heater and kept at a given temperature measured by a K-type thermocouple. The surface roughness of the AISI304 substrate was 22.8 nm measured using atomic force microscope (AFM) (SPM-9500J3, Shimadzu Co., Ltd. Tokyo, Japan) covering an area of 100 μm^2, no significant surface roughness and topography change along with the substrate temperature even heated up to 573 K.

The free falling apparatus is shown in Fig. 1. Droplet was heated and melted by radio-frequency heating equipment (RWN-1-20, Nihon Koshuha Co., Ltd., Kanagawa, Japan) prior to the falling. The substrate temperature was varied between 298 K (referred to as "room temperature" in this article) and 573 K, while ambient pressure was varied between 101.3 kPa (referred to as "atmospheric pressure" in this article) and 6.7 kPa, and the falling distance is 1000 mm. The droplet velocity

Table 1 Physical properties of Cu droplet

Density, ×10^3 kg/m^3	Viscosity, mNs/m^2	Conductivity, W/m · k	Heat capacity, J · mol^{-1} · K^{-1}	Melting point, K	Latent heat, J/g	Surface tension, mN/m
8.00	4.0	401	24.44	1356	209.28	1285

Table 2 Chemical compositions of AISI304 substrate (wt.%)

Alloy	C	Si	Mn	P	S	Ni	Cr	Bal.
SUS304	<0.08	<1.00	<2.00	<0.045	<0.03	8.00-10.50	18.00-20.00	Fe

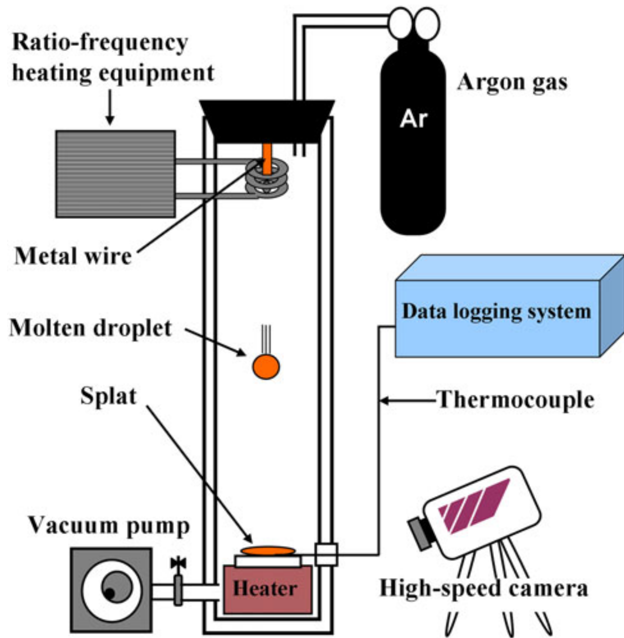

Fig. 1 Schematic of free falling experimental apparatus

Table 3 Dimensionless parameters of free falling droplet and thermal-sprayed particle

	Free falling droplet	Thermal-sprayed particle
Re number	2.39×10^{4}	2.13×10^{4}
Pe number	8.18×10^{-5}	7.27×10^{-5}
We number	278	8406

at impact was measured using laser sensor (LV-H300, Keyence, Co., Ltd., Osaka, Japan), it was 4.2 m/s in this study. Reynolds, Peclet, and Weber numbers (Ref 33-35) for both free falling droplets and thermal-sprayed particles are summarized in Table 3. Therefore, the experimental conditions were determined as equivalent Reynolds and Peclet numbers as practical thermal spray process, despite the different impact velocity and diameter of the droplets. All the free falling experiments were conducted in an argon atmosphere to eliminate oxidation.

2.2 Raw Materials and Thermal Spraying Apparatus

Commercially available Cu powders with a diameter of 75 μm or less (Kojundo Chemical Lab. Co., Ltd., Japan.) were thermally sprayed onto AISI304 substrates surface. The plates with dimensions of 20 × 20 × 6 mm were finally polished with 0.3 μm Al_2O_3 buff prior to spraying. Spraying work was conducted using low-pressure plasma spraying (LPPS), a SG-100 plasma torch (Praxair Surface Technologies, Indianapolis, IN, USA) was used. During deposition, the substrate surface was held vertically and spray gun was held horizontally so that the direction of droplet stream was perpendicular to the substrate surface.

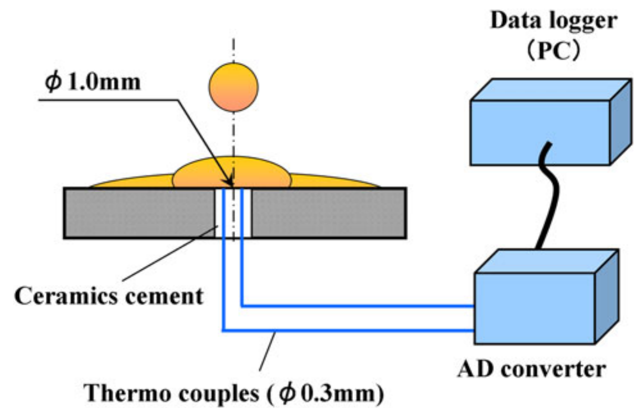

Fig. 2 Schematic of temperature data logging system

Splats were collected on the substrate by moving the shutter rapidly in one direction. Ambient pressure was set the same as free falling experiment, the spraying method in detail can be referred in our previous report (Ref 6, 8).

2.3 Evaluation Methods

Thermal history of the droplet on the substrate was measured in this study; the temperature sensor was set up on the substrate as shown in Fig. 2. A hole with a diameter of 1 mm was drilled at the center of substrate, J-type thermocouple (Okazaki Manufacturing Company, Kobe, Japan) with a diameter of 0.3 mm was inserted through this hole. A small amount of ceramic cement (Sumiseramu S-10A, Asahi Chemical Industry Co., Ltd., Wakayama, Japan) was forced into the hole, which also acted as an electrical insulator between the thermocouple and the substrate. The thermo electromotive force was converted to digital signal and recorded by data logging system (NI PCI6251, National Instruments Japan Corporation, Tokyo, Japan), and the temperature response time was less than 1 ms. Heichal et al. (Ref 26, 36) have given further details a similar method of measuring the temperature at interface of substrate-droplet in their study.

The splat top surface was observed using optical microscope (OM) (Eclipse LV100D, Nikon Co., Ltd., Tokyo, Japan). Tensile test was conducted to evaluate the adhesion strength of the individual splat on substrate. Jig ($d = 8$ mm) was bonded on the splat surface and tensile test was carried out by tensile tester (KS-501H, Attonic Co., Ltd., Aichi, Japan). Following this, splat bottom surface morphologies were captured by scanning electron microscope (SEM) (JSM-6390TY, Jeol Datum Ltd., Tokyo, Japan). ImageJ imaging software (National Institutes of Health, Washington, DC, USA) was employed to quantify pore size and distribution on the bottom surface of the splats. Degree of porosity was defined as pore area divided by total measurement area, the measuring method can be referred in the previous report (Ref 8, 37). While the periphery outline of the splat was captured by optical microscope. The circularity ratio of the splat was

calculated by ImageJ imaging software. The circularity ratio was defined in Eq 2

$$D_C = \frac{4 \cdot \pi \cdot S}{L^2} \quad \text{(Eq 2)}$$

where S and L are the surface area (m^2) and circumferential length (m), respectively. The circularity ratio D_C will be greater than 0 and less than or equal to 1. A long, thin shape has a circularity that approaches 0 and a circle has a circularity of 1.

For precisely observation of the flattening process of the droplet on the flat substrate, the spreading behavior of the molten droplet on substrate surface was captured by high speed camera (FASTCAM-ultima, Photron Co., Ltd., Tokyo, Japan). In order to observe the droplet impinging instant motion and capture the splat flattening behavior clearly, the frame grabber rate was set as 13,500 fps.

The morphologies of thermal spraying depositions in detail were observed using scanning electron microscope as well.

3. Results and Discussion

3.1 Splat Characteristics

Splat top surface morphologies of Cu droplets on AISI304 substrate obtained under designated conditions are shown in Fig. 3. From the figure, the splat collected on the substrate with room temperature under atmospheric pressure was a splash, and the splash fingers always connected with the center solidification area, whereas the splat morphology changes from splash-shape to a disk one with increasing substrate temperature, while the ambient pressure was kept at atmospheric pressure. The final diameter of the disk-shaped splat was smaller than the splash splat. Moreover, similar transition tendency was observed by reducing the ambient pressure in deposition chamber, while the substrate was kept at room temperature.

Figure 4 shows the splat bottom surface morphologies experimented at various substrate temperatures under atmospheric pressure. Splat center part is located in left side and rim part is shown in right side in the figure. Figure 4(a) shows the bottom surface of the splat collected on the substrate at room temperature. The pore distribution was different between center area and peripheral part of bottom surface. In the central area with 500 μm diameter, small independent pores can be observed and with metal flowing structure. On the other hand, metal flowing with elongated pore structure can be observed in outer part. It can be estimated that center area of the splat was formed under a higher impact pressure impingement condition compared with other part. Li et al. (Ref 38) proposed that the impact pressure can be very high and concentrates at a small contacting area and then spreads quickly with droplet flattening. The maximum pressure is located at the front of the droplet at an early stage of deformation, which drives the fluid moving quickly along substrate and results in lateral flow. This dynamic impact pressure spreads out and dissipates quickly with droplet flattening, the peak pressure reduces monotonically with flattening, and becomes negligible at the region where the flattening degree is larger than 2. Meanwhile, pore basically inhibits the heat transfer, because contact area of splat and substrate is decreased by the existence of pore at the interface. It is apparent from the figure that the pore density gradually decreases with increasing substrate

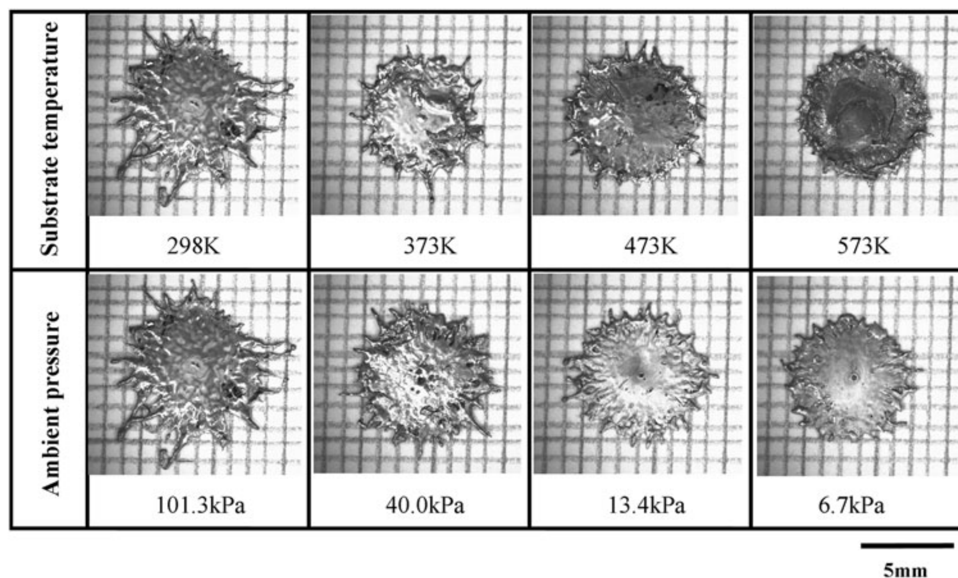

Fig. 3 Dependence of splat morphologies on substrate temperature and ambient pressure in deposition chamber (the chamber pressure was kept at atmospheric pressure when varied the substrate temperature, while no substrate heating was conducted when varied the ambient pressure)

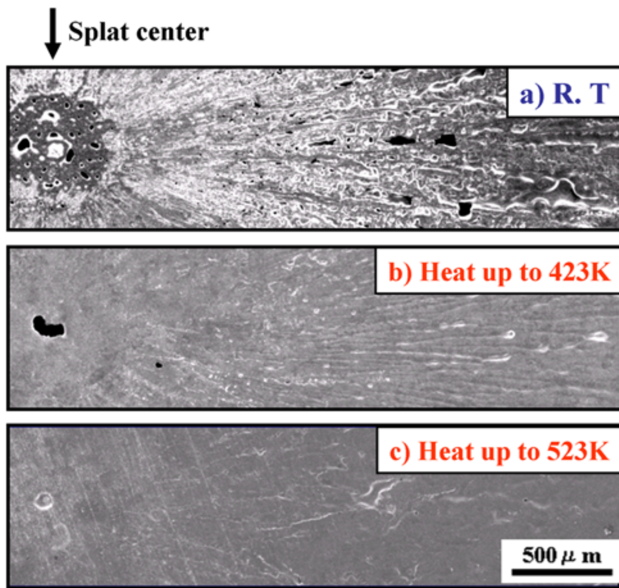

Fig. 4 Splat bottom surface morphologies by controlling substrate temperature

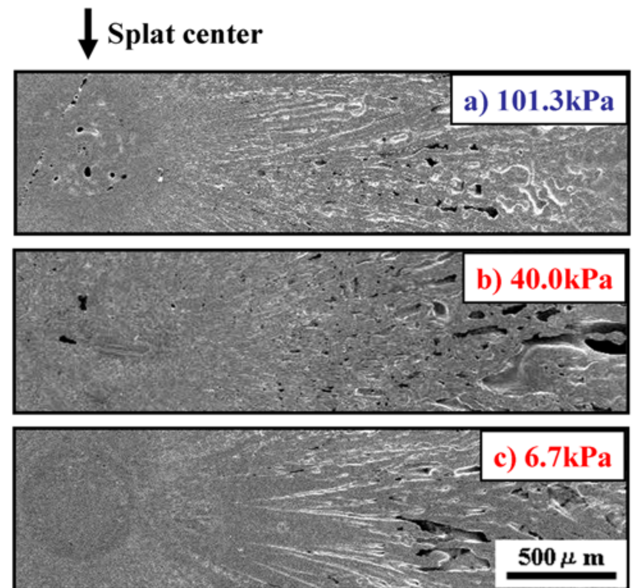

Fig. 5 Splat bottom surface morphologies by controlling ambient pressure in deposition chamber

temperature. Splat on the substrate kept at 523 K as shown in Fig. 4(c), almost no pore can be observed from the bottom surface view, and the solidification structure looks quite homogeneous, because substrate heating cleans the adsorption of contaminants, such as water vapor on the substrate surface, and decreases the ability of a surface to adsorb ambient vapors as proposed by McDonald et al. (Ref 19) in their study. The result indicates that the substrate heating improves the contact condition between splat and substrate and resultant better heat transfer can be given by the substrate heating.

The splat bottom surface morphologies experimented under various ambient pressures in deposition chamber are shown in Fig. 5, all the substrates were unheated. It is found that the pores gradually decrease with the decrease of ambient pressure. However, this tendency can be found only at central part of the splat, but pores still exist at peripheral part even the ambient pressure was lowered to 6.7 kPa as shown in Fig. 5(c). Similar dependence of splat pores on ambient pressure for the thermal-sprayed particles has already presented by the authors (Ref 8). The result indicates that ambient pressure affects similarly to the heat transfer between splat and substrate as the substrate temperature.

In general, when a molten droplet impacts on a polished substrate surface, the lateral flattening of the liquid fluid along the substrate surface takes place. The dynamic impact pressure toward the substrate surface will be generated to keep the fluid flowing along the substrate surface (Ref 39). The impact pressure also forces adsorbed gas/condensation trapped between the droplet and the substrate to rapidly dissolve into the molten metal. The rapid decompression to ambient pressure supersaturates the gas dissolved in the molten metal and causes high nucleation rates of bubbles. Solidification occurs within several

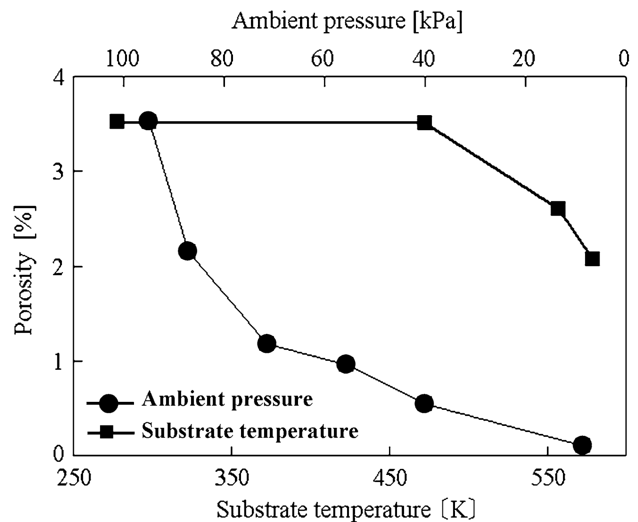

Fig. 6 Dependence of splat porosity on substrate temperature and ambient pressure in deposition chamber

microseconds, the bubbles grow somewhat and are pulled by liquid motion before being "frozen" into the structure. Finally, the pores are formed (Ref 40).

The porosity was measured by ImageJ imaging software for entire bottom surface of each splat as shown in Fig. 6. According to the result, it was found that the substrate temperature has a strong effect on splat porosity, the porosity decrease rapidly with the increase of substrate temperature. In other words, the absence/presence of pores in the splat is a function of substrate temperature (Ref 19). In particular, porosity decreased to less than 0.1% on the substrate with highest temperature of 573 K.

Ambient pressure in deposition chamber also has a similar effect on porosity decrease, but the changing is not so remarkable. In this case, porosity definitely decreased to around 2% at 6.7 kPa.

Actually, most metal surfaces exposed to air atmosphere will be oxidized to cover a thin oxide film with a thickness over several nanometers. The adsorption to a metal surface will occur usually through the oxide film of the metal at atmospheric pressure. However, McDonald et al. (Ref 19) reported that even by substrate preheating, the oxide film thickness is too low for the effect of thermal contact resistance to be significant. Tran and Hyland (Ref 41) also proposed that the splat morphology was not influenced by the thickness of the oxide layer of the substrate surface by simulation method. In nature, water and some kinds of gases may cover the substrate surface in atmospheric condition. Especially, water molecules easy to gather on substrate surface as condensates (Ref 39, 42). These adsorbates and condensates may become origins to produce the pore at splat bottom surface observed. Water condensate evaporates from substrate surface by substrate heating or/and ambient pressure reduction (Ref 6, 8, 20). The fact that porosity of the splat begun to decrease significantly at temperature of 373 K as shown in Fig. 6 implies that water desorption may be a trigger for that, which likely to occur near 373 K in atmospheric pressure condition.

As thermal-sprayed coating is composed of lots of particles flattened, in other words, splat is unit cell for the entire coating build-up, splat adhesion character is effective for evaluating the coating adhesion strength. Pershin et al. (Ref 18) found that the coating adhesion strength increases with increasing substrate temperature. However, no study of the relationship between adhesion strength of single splat and substrate temperature has been reported yet. Therefore, the adhesion strength of individual splat on the substrate under designated conditions was measured in this study. Also, the circularity ratio of the individual free falling splat was evaluated as well. The dependence of individual splat adhesion strength and circularity ratio on substrate temperature is summarized in Fig. 7. It was found that the adhesion strength increases with increasing substrate temperature, a remarkable increasing tendency can be obtained on the substrate with higher heating temperature, which corresponded well to that of the coating adhesion strength. According to the figure, the circularity ratio of the individual splat increases with increasing substrate temperature, as well. However, the slope of the curve is shaper at the substrate with higher temperature than the one with lower temperature, which indicates that the increase of circularity ratio become significantly along with the substrate temperature.

Similarly, Fig. 8 shows the dependence of adhesion strength and circularity ratio of the individual splat on the ambient pressure in deposition chamber. Adhesion strength increases with ambient pressure decrease and circularity ratio also increases correspondingly. Both the values have similar changing tendency by controlling the ambient pressure, but the adhesion strength in this case is much smaller than those of substrate temperature change.

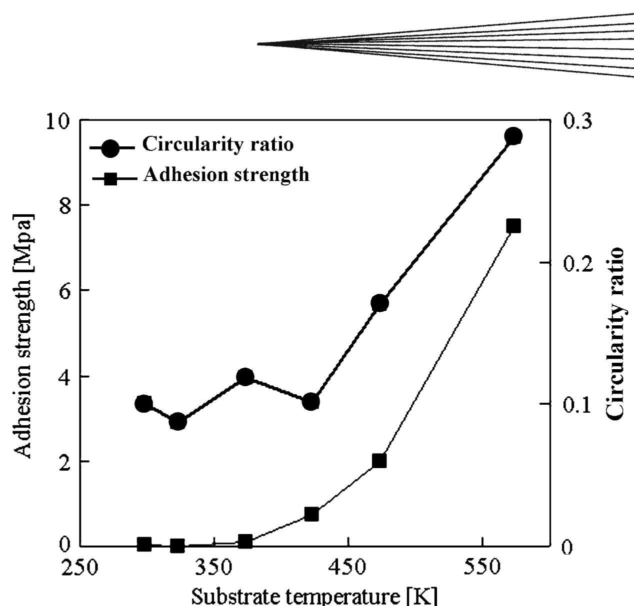

Fig. 7 Dependence of splat adhesion and circularity ratio on substrate temperature

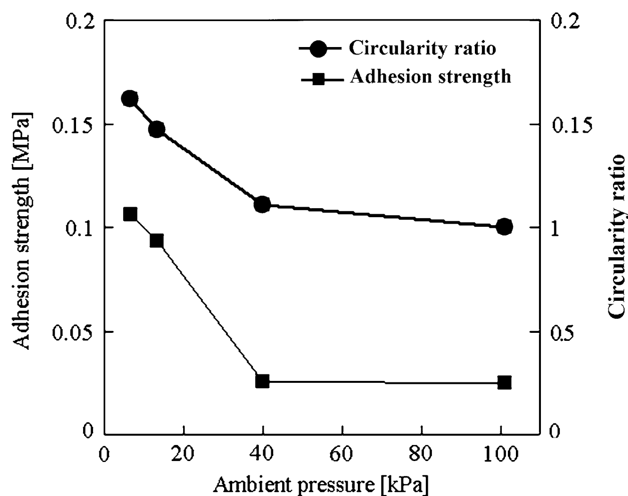

Fig. 8 Dependence of splat adhesion and circularity ratio on ambient pressure in deposition chamber

The result indicates that contact conditions at bottom surface of the splats at pressure reduced conditions are not so improved significantly. It might be caused by different cleaning effect of the substrate surface and different wettability as those of the substrate temperature. However, similar changing tendency in adhesion strength and circularity ratio was confirmed.

3.2 Evaluation of Heat Transfer Between Molten Droplet and Substrate Surface

To clarify the effect of substrate temperature and ambient pressure on heat transfer at interface between molten droplet and substrate surface, splat temperature history was measured under the designated conditions. As thermocouple junction can be connected by molten metal

of the splat, the temperature in splat bottom part was recorded since droplet impinged onto substrate surface. The slope of this splat temperature history curve, dT/dt, was defined to be the cooling rate of the splat.

The temperature histories and corresponding cooling rates in the splats kept at various substrate temperatures are summarized in Fig. 9. All the measurements were conducted at atmospheric pressure, and substrate temperatures were room temperature, 423 and 523 K, respectively. Temperature elevation was recognized at first stage of splat impingement at all substrate heating conditions, indicating that the temperature of outside shell of the splat was lower than its inside. In the next stage, splat cooling started with splat flattening. Splat temperature elevation occurred again only on the substrate kept at 523 K. This elevated temperature period can be estimated as a plateau in the solidification. The plateau appeared at 1000 K in this case, i.e., it was slightly lower than the melting point of the droplet material. It means that droplet was super cooling condition when impinged onto the substrate.

The cooling rate was calculated from the splat temperature curve under the designated conditions as shown in Fig. 9(b). According to the result, it is found that the splat cooling rates on heated substrates were remarkably higher than those substrates with room temperature, and increases with substrate heating temperature, increasing from 4.4×10^3 K/s on the substrate with room temperature to 2.1×10^4 K/s on the substrate heated up to 523 K. Similar result has been proposed while some kinds of micrometer-sized particles were thermally sprayed onto flat substrate surfaces (Ref 19, 26, 43, 44). Namely, it is opposite tendency from the theory of Newtonian cooling (Ref 45). The measurement result indicates the heat transfer between molten droplet and substrate is not decided by only difference of temperature between splat and substrate, but other factors may have a strongly effect.

The results of temperature histories and corresponding cooling rates in the splats kept at various ambient pressures in deposition chamber are shown in Fig. 10. All the measurements were conducted on nonheated substrate, and ambient pressure was 101.3, 40.0, and 6.7 kPa, respectively. According to Fig. 10(b), it is found that cooling rate in the splat increases with decrease of ambient pressure, increasing from 4.4×10^3 K/s on the substrate under atmospheric pressure to 1.1×10^4 K/s on the substrate located at an ambient pressure of 6.7 kPa.

Thus, similar tendency in ambient pressure as substrate temperature was recognized, indicating that equivalent effect on the heat transfer character can be given both by substrate temperature and by ambient pressure. The cause of the lower cooling rate on the substrate at room temperature and under atmospheric pressure is probably the adsorbates and condensates. Good contact can be

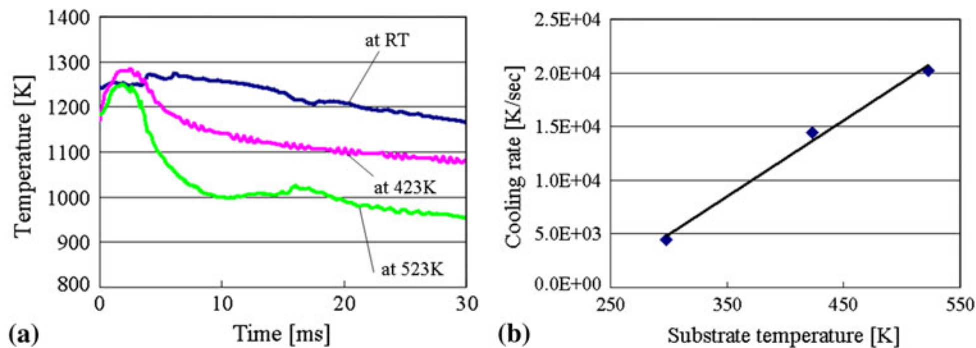

Fig. 9 Droplet temperature history and cooling rate by controlling substrate temperature

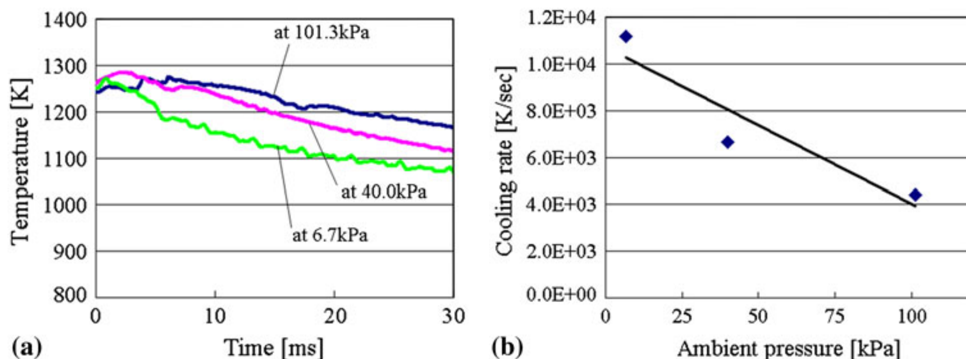

Fig. 10 Droplet temperature history and cooling rate by controlling ambient pressure in deposition chamber

obtained by removing the adsorbed/gas condensation through substrate heating or ambient pressure reduction (Ref 8, 25, 46), thereby, the heat transfer between the molten droplet and the substrate surface was enhanced, corresponding with higher cooling rate, and finally affect the splat formation.

Generally, the influence of substrate temperature on the cooling rate, splat porosity, and adhesion strength seems much stronger than that of ambient pressure factor. When the substrate was heated up to the designated temperature, desorption of the adsorbed/gas condensation took place immediately (Ref 39, 42). Meanwhile, the substrate surface will be oxidized to cover a thin oxide film with a thickness over several nanometers. In particular, the previous studies indicated that the surface roughness of the once heated substrate tend to be remarkably bigger than those of the substrate as polished condition, more valleys and peaks can be observed (Ref 6, 47). Wenzel's law proposed that a small increase of surface roughness would lead to a reduction of the contact angle (Ref 48). In other words, surface roughness increase in nanoscale promotes the wetting, Uelzen and Muller (Ref 49) also verified the result in their study. On the other hand, as the substrate material used in this study was stainless steel, and the substrates were stored for appropriate periods at room temperature in a dry condition, it is estimated that no significant oxidation change by reducing the ambient pressure. Therefore, no significant topography and surface roughness change took place, only the adsorption/desorption of the adsorbates and condensates changed by controlling the ambient pressure. Consequently, the influence of substrate temperature is stronger than that of the ambient pressure on the flattening behavior of the molten droplet in some cases, but the tendency is quite similar.

3.3 Flattening Process of Molten Droplet on Substrate Surface

The flattening process of Cu droplet on AISI304 substrate was observed using high speed camera as presented in Fig. 11. According to the results, flattening behavior was almost similar till 0.30 ms after the impingement under the designated conditions. However, difference in flattening degree begun to be observed from 0.44 ms, i.e., walled-rim structures were formed both on the substrate heated and ambient pressure reduced conditions. It cannot be observed on substrate located at room temperature and atmospheric pressure, which was defined as base condition in the figure. Moreover, walled-rim splat finished its flattening at 1.04 ms and kept its shape, while splashing occurred in the base condition at the same time. In other words, the splash splat flattened rapidly. It was found that the final flattening degree of the splash splat was larger than those of the disk-shaped splat, similar result was proposed using Ni as the droplet material (Ref 25).

These results indicate that substrate heating and pressure reduction may enhance the wetting condition during splat flattening, and then improve the contact condition at splat/substrate interface. Therefore, substrate temperature and ambient pressure in deposition chamber have an equivalent effect on wetting and intimate contact at interface between droplet and substrate surface. Even not enough evidences of the effect of wetting, especially the

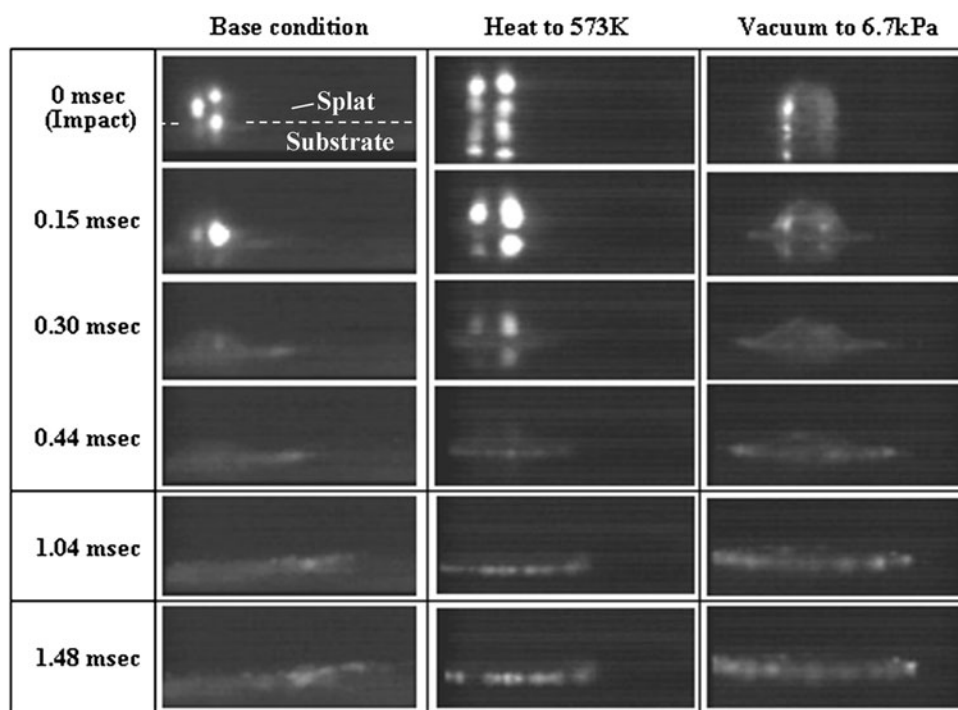

Fig. 11 High speed camera observation of Cu droplet on AISI304 substrate under designated conditions

dynamic wetting on the flattening can be provided with the current technology, but there is no doubt that wetting likely has an important role in the droplet flattening process.

3.4 Domination in Flattening of Molten Droplet

When the molten droplet impinged onto the substrate surface, radial flattening of the liquid metal occurs initially and then solidification occurs. Cooling rate in splat bottom part is undoubtedly higher than that in splat top surface, because the heat transfer preferentially occurs at splat/substrate interface than splat/ambient air interface. Therefore, the solidification starts from bottom surface of the splat. It is also indicated that free falling droplet has enough kinetic energy for the splashing after impingement onto substrate surface. If the splat cooling at bottom surface was restrained, the inside of the droplet solidifies slowly and the viscosity increase is small, and splat body splashes away on the flat substrate surface.

On the other hand, by substrate heating or ambient pressure reduction, the contact condition is good, owing to the good wettability, hence heat transfer between flattening splat and substrate was enough higher, splat solidification occurs significantly at bottom surface due to the enhanced cooling rate, and it propagates so quickly to its surface. Such quick temperature decrease brings about the remarkable increase of viscosity of the material. Thus, the initial kinetic energy is consumed so effectively as viscous energy and solidification (Ref 25). Disk-shaped splat can be attributed essentially to good contact at splat/substrate interface, in other words, good wetting condition.

As a confirmation of the meaning of this investigation on thermal spraying process, Cu particles were thermally sprayed onto mirror-polished AISI304 substrate surface at various ambient pressures ranging from 101.3 to 6.7 kPa. Collected splats were examined using SEM as shown in Fig. 12. It is clearly observed that with the reduction of ambient pressure, the splat pattern changed from the form with splashing to the one without splashing. Splash splat was obtained at atmospheric pressure, forming a fragmented splat with irregular edge, the splash splat consists of a small central disk as well as a splash region, surrounded by a ring of fragments. While the ambient pressure was lowered to 40.0 kPa, only few short and smooth splash fingers were found around the central part as well. While disk-shaped splat was obtained at low pressure condition of 6.7 kPa, nearly no splash fingers exist around the center solidification area. The shape of the splashing itself was different from the free falling splat, however, the splat of the thermal-sprayed particles showed similar changing tendency as in the free falling experiment, despite the different impact velocity and diameter of the droplets. Also, Sampath and Herman (Ref 50) reported that more contiguous Ni splats were formed in a reduced pressure chamber than at atmospheric pressure.

Moreover, existence of a similar transition phenomenon in a flattening behavior of the thermal-sprayed particles on the flat substrate surface by controlling substrate temperature was introduced by the authors (Ref 5, 6). The splat shape change transitionally from a splash shape to a disk one by substrate preheating. All the results showed similar changing tendency as free falling experiment. Thus, investigation of the thermal spray process through observation on individual splat behavior is meaningful.

4. Conclusions

To evaluate the effects of substrate temperature and ambient pressure on flattening and solidification behavior of free falling droplet, millimeter-sized molten Cu droplets were collected on AISI304 substrate surface. The heat transfer at interface between molten droplet and substrate surface was systematically investigated. Furthermore, the spreading behavior of molten droplet on substrate surface was observed using high speed camera. The results obtained in this study are summarized as follows:

(1) The porosity at splat bottom surface decreased remarkably with increasing substrate temperature and reducing ambient pressure. Consequently, substrate temperature and ambient pressure have equivalent effect on contact condition at interface between droplet and substrate surface. The wetting of substrate surface by molten droplet during splat flattening may be enhanced by substrate heating and pressure reduction.

(2) Due to the improved droplet-substrate contact, the heat transfer should be enhanced, followed by the

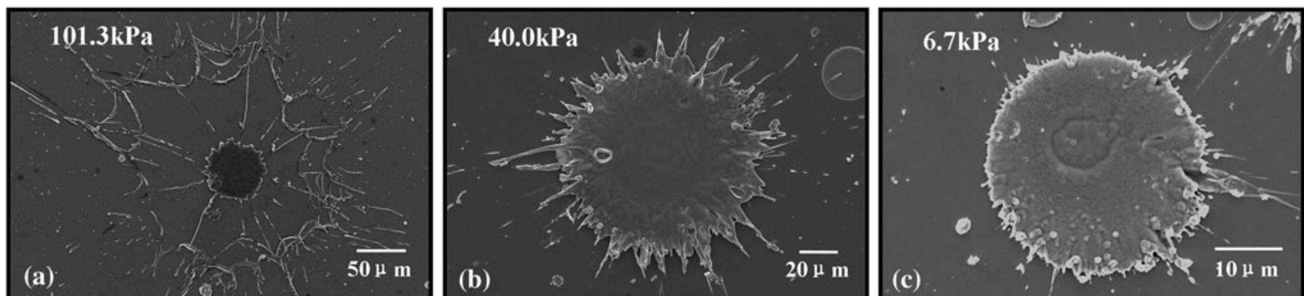

Fig. 12 Top morphologies of Cu particles thermally sprayed onto AISI304 substrate by controlling ambient pressure in deposition chamber

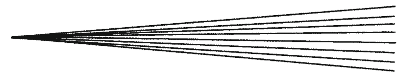

improved cooling rate. If heat transfer between flattening splat and substrate was enough higher, splat solidification occurs significantly at bottom surface, and it propagates so quickly to its surface. Such quick temperature decrease brings about the remarkable increase of viscosity of the droplet. Thus, the initial kinetic energy is consumed so effectively as viscous energy and solidification. Therefore, disk-shaped splat can be attributed essentially to good contact at splat/substrate interface, in other words, good wetting at interface. On the contrary, splash splat formed.

(3) The adhesion strength and circularity ratio of the individual splat were enhanced by both substrate heating and reducing the ambient pressure, its dependence on the substrate temperature and ambient pressure corresponded well to that of the splat shape.

(4) The shapes of splats in free falling experiment showed similar changing tendency as thermal-sprayed particles. Thus, investigation of the flattening behavior of individual splat on flat substrate surface is significantly meaningful for the practical usage of the thermal spray process.

Acknowledgments

The authors would like to acknowledge Mr. Y. Ebisuno and T. Matsuda for their assistance and valuable discussions in the experiments. This research was partially supported both by the Grant-in-Aid for Scientific Research of the Ministry of Education, Science, Culture and Sports in Japan, and by a special research fund in Toyohashi University of Technology.

References

1. M.L. Thorpe, Thermal Spray Industry in Transition, *Adv. Mater. Process*, 1993, **143**(5), p 50-61
2. F. Kassabji, G. Jacq, and J.P. Durand, Thermal Spray Applications for the Next Millenium: A Business Development Perspective, *Proceedings of the International Thermal Spraying Conference 1998*, C. Coddet, Ed., May 25-29, 1998 (Nice, France), ASM International, Materials Park, OH, 1998, p 1677-1680
3. M. Ducos and J.P. Durand, Thermal Coatings in Europe, Business Prospection, *Proceedings of the International Thermal Spraying Conference 2001*, C.C. Berndt, K.A. Khor, and E.F. Lugscheider, Ed., May 25-29, 2001 (Singapore), ASM International, Materials Park, OH, 2001, p 1267-1271
4. M. Fukumoto, H. Hayashi, and T. Yokoyama, Relationship Between Particle's Splat Pattern and Coating Adhesive Strength of HVOF Sprayed Cu-Alloy, *J. Jpn. Therm. Spray Soc.*, 1995, **32**(3), p 149-156 (in Japanese)
5. M. Fukumoto, S. Katoh, and I. Okane, Splat Behavior of Plasma Sprayed Particles on Flat Substrate Surface, *Proceedings of the International Thermal Spray Conference 1995*, A. Ohmori, Ed., May 22-26, 1995 (Kobe, Japan), ASM International, Materials Park, OH, 1995, p 353-358
6. M. Fukumoto, K. Yang, T. Yasui, and M. Yamada, Control of Thermal Spray Process through Observation on Individual Splat Behavior, *J. Solid Mech. Mater. Eng.*, 2010, **4**(2), p 107-118
7. M. Vardelle, A. Vardelle, A.C. Leger, P. Fauchais, and D. Gobin, Influence of Particle Parameters at Impact on Splat Formation and Solidification in Plasma Spraying Processes, *J. Therm. Spray Technol.*, 1995, **4**(1), p 50-58
8. K. Yang, K. Tomita, M. Fukumoto, M. Yamada, and T. Yasui, Effect of Ambient Pressure on Flattening Behavior of Thermal Sprayed Particles, *J. Therm. Spray Technol.*, 2009, **18**(4), p 510-518
9. M. Fukumoto, Y. Tanaka, and E. Nishioka, Flattening Problem of Thermal Sprayed Particles, *Mater. Sci. Forum*, 2004, **449-452**, p 1309-1312
10. M. Fukumoto, M. Shiiba, H. Kaji, and T. Yasui, Three-Dimensional Transition Map of Flattening Behavior in the Thermal Spray Process, *Pure Appl. Chem.*, 2005, **77**(2), p 429-442
11. M. Fukumoto, T. Yamaguchi, M. Yamada, and T. Yasui, Splash Splat to Disk Splat Transition Behavior in Plasma-Sprayed Metallic Materials, *J. Therm. Spray Technol.*, 2007, **16**(5-6), p 905-912
12. J. Madjeski, Solidification of Droplets on a Cold Surface, *Int. J. Heat Mass Transf.*, 1976, **19**, p 1009-1013
13. H. Fukanuma, A Porosity Formation Flattening Model of an Impinging Molten Particle in Thermal Spray Coatings, *J. Therm. Spray Technol.*, 1994, **3**(1), p 33-44
14. R. Dhiman, A. McDonald, and S. Chandra, Predicting Splat Morphology in a Thermal Spray Process, *Surf. Coat Technol.*, 2007, **201**, p 7789-7801
15. S. Chandra and P. Fauchais, Formation of Solid Splats During Thermal Spray Deposition, *J. Therm. Spray Technol.*, 2009, **18**(2), p 148-180
16. A.T.T. Tran, S. Brossard, M.M. Hyland, B.J. James, and P. Munroe, Evidence of Substrate Melting of NiCr Particles on Stainless Steel Substrate by Experimental Observation and Simulations, *Plasma. Chem. Plasma Process.*, 2009, **29**, p 475-495
17. C. Moreau, P. Gougeon, and M. Lamontagne, Influence of Substrate Preparation on the Flattening and Cooling of Plasma-Sprayed Particles, *J. Therm. Spray Technol.*, 1995, **4**(1), p 25-33
18. V. Pershin, M. Lufitha, S. Chandra, and J. Mostaghimi, Effect of Substrate Temperature on Adhesion Strength of Plasma-Sprayed Nickel Coatings, *J. Therm. Spray Technol.*, 2003, **12**(3), p 370-376
19. A. McDonald, C. Moreau, and S. Chandra, Effect of Substrate Oxidation on Spreading of Plasma-Sprayed Nickel on Stainless Steel, *Surf. Coat Technol.*, 2007, **202**, p 23-33
20. K. Yang, T. Usami, Y. Ebisuno, K. Tanaka, M. Fukumoto, T. Yasui, and M. Yamada, Study of Wetting on Flattening Behavior of Thermal Sprayed Particles, *Proceedings of the 4th Asian Thermal Spray Conference (ATSC2009)*, chaired by C.J. Li, October 22-24, 2009 (Xi'an, China), p 226-231
21. C. Mundo, M. Sommerfeld, and C. Tropea, Droplet-Wall Collisions: Experimental Studies of the Deformation and Breakup Process, *Int. J. Multiphase Flow*, 1995, **21**(2), p 151-173
22. P. Fauchais, M. Fukumoto, A. Vardelle, and M. Vardelle, Knowledge Concerning Splat Formation: An Invited Review, *J. Therm. Spray Technol.*, 2004, **13**(3), p 337-360
23. C. Escure, M. Vardelle, A. Vardelle, and P. Fauchais, Visualization on the Impact of Drops on a Substrate in Plasma Spraying: Deposition and Splashing Modes, *Proceedings of the International Thermal Spraying Conference 2001*, C.C. Berndt, K.A. Khor, and E.F. Lugscheider, Ed., May 25-29, 2001 (Singapore), ASM International, Materials Park, OH, 2001, p 805-812
24. H. Li, S. Costil, H.L. Liao, C.J. Li, M. Planche, and C. Coddet, Effects of Surface Conditions on the Flattening Behavior of Plasma Sprayed Cu Splats, *Surf. Coat Technol.*, 2006, **200**, p 5435-5446
25. M. Fukumoto, E. Nishioka, and T. Matsubara, Flattening and Solidification Behavior of a Metal Droplet on a Flat Substrate Surface Held at Various Temperatures, *Surf. Coat Technol.*, 1999, **120-121**, p 131-137
26. Y. Heichal and S. Chandra, Predicting Thermal Contact Resistance Between Molten Metal Droplets and a Solid Surface, *J. Heat Transf.*, 2005, **127**, p 1269-1275
27. M. Pasandideh-Fard, S. Chandra, and J. Mostaghimi, A Three-Dimensional Model of Droplet Impact and Solidification, *Int. J. Heat Mass Transf.*, 2002, **45**, p 2229-2242
28. S.D. Aziz and S. Chandra, Impact, Recoil and Splashing of Molten Metal Droplets, *Int. J. Heat Mass Transf.*, 2000, **43**, p 2841-2857

Peer Reviewed

29. R.G. Azar, Z. Yang, S. Chandra, and J. Mostaghimi, Impact of Molten Metal Droplets on the Tip of a Pin Projecting From a Flat Surface, *Int. J. Heat Fluid Flow*, 2005, **26**, p 334-347
30. M. Pasandideh-Fard, R. Bhola, S. Chandra, and J. Mostaghimi, Deposition of Tin Droplets on a Steel Experiments Plate: Simulations and Experiments, *Int. J. Heat Mass Transf.*, 1998, **41**, p 2929-2945
31. Y. Tanaka, S. Yoshida, and R. Kawase, Effect of Impact Velocity and Preheated Substrate Temperature on Flattening and Solidifying Behavior of Free Falling Metal Droplet, *J. Jpn. Therm. Spray Soc.*, 2010, **47**(2), p 54-60 (in Japanese)
32. L. Battezzati and A.L. Greer, The Viscosity of Liquid Metals and Alloys, *Acta Metall.*, 1989, **37**(7), p 1791-1802
33. S.G.G. Stokes, On the Effect of the Internal Friction of Fluids on the Motion of Pendulums, *Trans. Camb. Philos. Soc.*, 1851, **9**, p 8-106
34. O. Reynolds, An Experimental Investigation of the Circumstances Which Determine Whether the Motion of Water Shall be Direct or Sinuous, and of the Law of Resistance in Parallel Channels, *Philos. Trans. R. Soc.*, 1883, **174**, p 935-982
35. N. Rott, Note on the History of the Reynolds Number, *Annu. Rev. Fluid Mech.*, 1990, **22**, p 1-11
36. Y. Heichal, S. Chandra, and E. Bordatchev, A Fast-Response Thin Film Thermocouple to Measure Rapid Surface Temperature Changes, *Exp. Therm Fluid Sci.*, 2005, **30**(2), p 153-159
37. M. Qu and A. Gouldstone, On the Role of Bubbles in Metallic Splat Nanopores and Adhesion, *J. Therm. Spray Technol.*, 2008, **17**(4), p 486-494
38. C.J. Li and J.L. Li, Transient Contact Pressure During Flattening of Thermal Spray Droplet and its Effect on Splat Formation, *J. Therm. Spray Technol.*, 2004, **13**(2), p 229-238
39. C.J. Li and J.L. Li, Evaporated-Gas-Induced Splashing Model for Splat Formation During Plasma Spraying, *Surf. Coat Technol.*, 2004, **184**, p 13-23
40. M. Qu, Y. Wu, V. Srinivasan, and A. Gouldstone, Observations of Nanoporous Foam Arising From Impact and Rapid Solidification of Molten Ni Droplets, *Appl. Phys. Lett.*, 2007, **90**, p 254101-1-254101-3
41. A.T.T. Tran and M.M. Hyland, The Role of Substrate Surface Chemistry on Splat Formation During Plasma Spray Deposition by Experiments and Simulations, *J. Therm. Spray Technol.*, 2009, **19**(1-2), p 11-23
42. V.E. Henrich and P.A. Cox, *The Surface Science of Metal Oxides*, Cambridge University Press, Cambridge, New York, 1994
43. A. McDonald, M. Lamontagne, C. Moreau, and S. Chandra, Impact of Plasma-Sprayed Metal Particles on Hot and Cold Glass Surfaces, *Thin Solid Films*, 2006, **514**, p 212-222
44. A. McDonald, C. Moreau, and S. Chandra, Thermal Contact Resistance Between Plasma Sprayed Particles and Flat Surfaces, *Int. J. Heat Mass Transf.*, 2007, **50**, p 1737-1749
45. R.H.S. Winterton, Newton's Law of Cooling, *Contemp. Phys.*, 1999, **40**(3), p 205-212
46. X. Jiang, Y. Wan, H. Herman, and S. Sampath, Role of Condensates and Adsorbates on Substrate Surface on Fragmentation of Impinging Molten Droplets During Thermal Spray, *Thin Solid Films*, 2001, **385**, p 132-141
47. M. Fukumoto, H. Nagai, and T. Yasui, Influence of Surface Character Change of Substrate Due to Heating on Flattening Behavior of Thermal Sprayed Particles, *J. Therm. Spray Technol.*, 2006, **15**(4), p 759-764
48. R.N. Wenzel, Resistance of Solid Surfaces to Wetting by Water, *Ind. Eng. Chem.*, 1936, **28**(8), p 988-994
49. T. Uelzen and J. Muller, Wettability Enhancement by Rough Surfaces Generated by Thin Film Technology, *Thin Solid Films*, 2003, **434**, p 311-315
50. S. Sampath and H. Herman, Rapid Solidification and Microstructure Development During Plasma Spray Deposition, *J. Therm. Spray Technol.*, 1996, **5**(4), p 445-456